Supporting Information

Hailfinger et al. 10.1073/pnas.1105020108

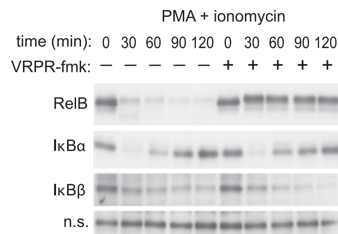

Fig. S1. IκBα and IκBβ degradation is not affected by Malt1 inhibition. Jurkat T cells were pretreated for 30 min with 75 μM of the Malt1 inhibitor VRPR-fmk or solvent control (DMSO) and then stimulated using PMA and ionomycin for the indicated time points. A nonspecific band serves as loading control. VRPR-fmk efficiently inhibited degradation of RelB but had no effect on IκBα or IκBβ degradation. Data are representative of three independent experiments.

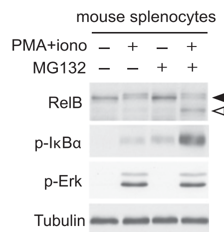

Fig. S2. RelB cleavage in mouse splenocytes. Mouse splenocytes were pretreated for 30 min with 5 μM MG132 or solvent control (DMSO). Cells were stimulated using PMA and ionomycin for 1 h. In the presence of MG132 the RelB fragment can be detected in activated splenocytes. Analysis of Erk phosphorylation (p-Erk) serves as stimulation control. Efficiency of MG132-mediated proteasome inhibition was controlled by assessing the levels of phosphorylated IkBa (p-IkBa). Data are representative of three independent experiments. Black and open arrowheads indicate uncleaved and cleaved forms, respectively, of RelB.

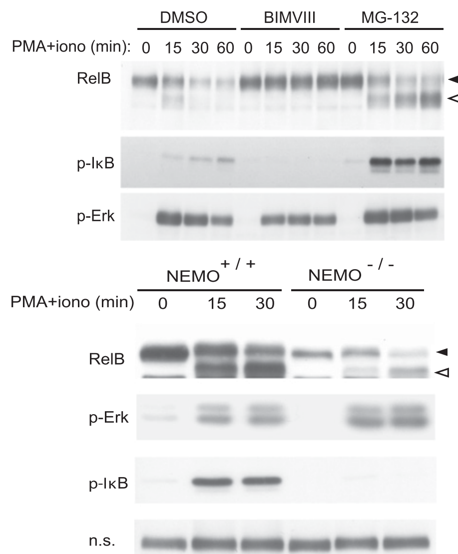

Fig. S3. RelB cleavage is dependent on PKC, but not on IKK activity. (*Upper*) Jurkat T cells were pretreated for 30 min with the pan-PKC inhibitor BIM VIII, the proteasome inhibitor MG132, or solvent alone (DMSO) before stimulation using PMA and ionomycin for the indicated times. Postnuclear lysates were analyzed by Western blotting as indicated. Note that BIM VIII inhibits induction of RelB cleavage, whereas MG132 inhibits the degradation of the newly generated RelB cleavage fragment. (*Lower*) Nemo-deficient and parental cells were treated with MG132 for 30 min before stimulation with PMA and ionomycin and post-nuclear lysates were analyzed by Western blotting as indicated. Nemo-deficient cells express lower levels of RelB, but still allow stimulation-induced RelB cleavage. Black and open arrowheads indicate uncleaved and cleaved forms, respectively, of RelB. A nonspecific (n.s.) band serves as loading control (*Lower*). Data are representative of two independent experiments.

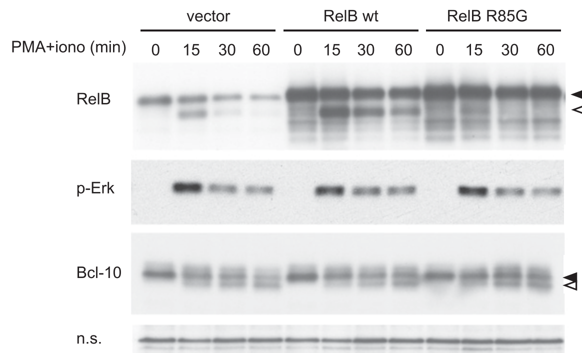

Fig. S4. RelB R85G is not cleaved in Raji B cells. Raji cells stably transduced with the WT or R85G mutated form of RelB were stimulated with PMA and ionomycin for the indicated times, and postnuclear lysates analyzed by Western blotting using anti-RelB, anti–Bcl-10, anti–p-IκBα, and anti–p-ERK. In contrast to the WT form, the R85G mutant of RelB is not cleaved in activated Raji cells. Data are representative of at least three independent experiments. Black and open arrowheads indicate uncleaved and cleaved forms.

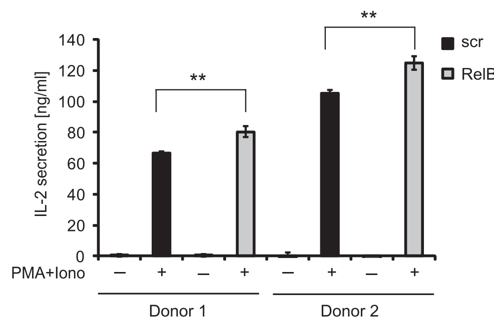

Fig. S5. RelB silencing in CD45RA^{+} cells results in increased IL-2 secretion upon PMA/ionomycin stimulation. CD45RA^{+} cells were isolated from human blood samples and electroporated with RelB-specific (RelB) or scrambled (scr) siRNA. Forty-eight hours after transfection, the cells were stimulated with PMA/ionomycin overnight and IL-2 levels were quantified by ELISA. Data are representative of two independent experiments. Statistical significance was calculated by Student's *t* test (***P* value <0.005).

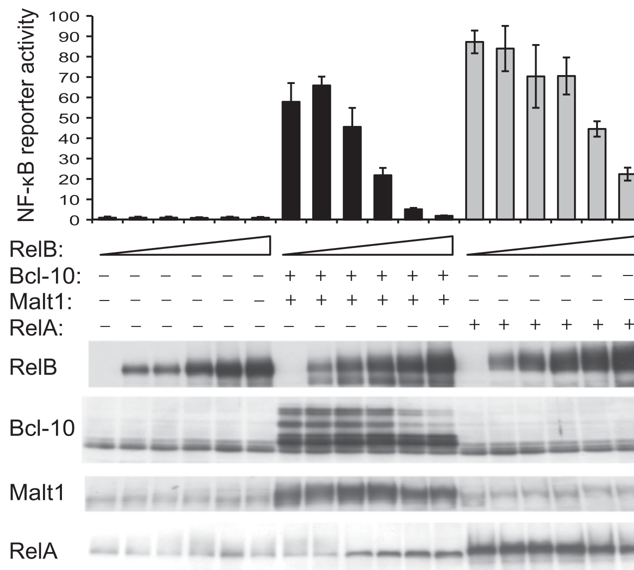

Fig. S6. RelB inhibits NF-κB activity in 293T cells. 293T cells were transfected with the indicated expression constructs and assessed 24 h later for NF-κB activation by luciferase reporter assay. The corresponding expression level of the constructs is shown below by Western blot. Note that RelB overexpression inhibits NF-κB activation by either Malt1 and Bcl-10 or RelA. Data are representative of two independent experiments.

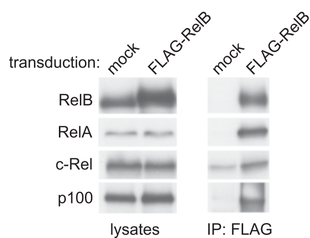

Fig. S7. RelA and c-Rel coimmunoprecipitate with FLAG-tagged RelB in Jurkat cells. Jurkat cells were stably transduced with an expression construct of FLAG-tagged RelB or empty vector. FLAG-tagged RelB was immunoprecipitated from postnuclear lysates using anti-FLAG sepharose (M2; Sigma). The lysate and the immunoprecipitate were analyzed for the presence of RelB, RelA, c-Rel, and p100 as indicated. FLAG-RelB associates constitutively with p100, but also with RelA, and to a lesser extent, with c-Rel (that shows some nonspecific binding to beads used for immunoprecipitation). Data are representative of three independent experiments.

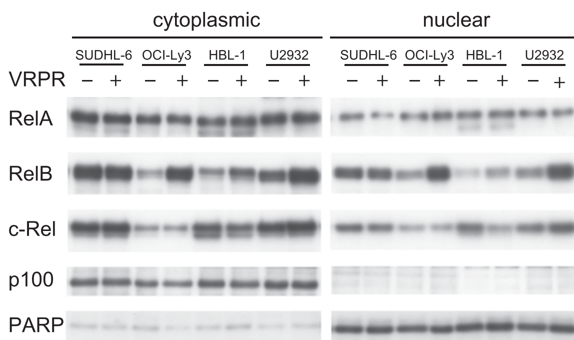

Fig. S8. Malt1 inhibition results in increased cytoplasmic and nuclear RelB levels in DLBCL cells. One GCB (SUDHL-6) and three ABC DLBCL (OCI-Ly3, HBL-1, and U2932) cell lines were treated with 75 μM VRPR-fmk or solvent control for 48 h. After cell fractionation, protein content was quantified by Bradford assay. Equal amounts of cytoplasmic and nuclear fractions were analyzed by WB using the indicated primary antibodies. To verify the purity of the fractions, the levels of p100 (cytoplasmic marker) and PARP (nuclear marker) were assessed. Note that inhibition of Malt1 by VRPR-fmk results in an increase in both cytoplasmic and nuclear levels of RelB in ABC DLBCL, which are characterized by constitutive Malt1 activity.

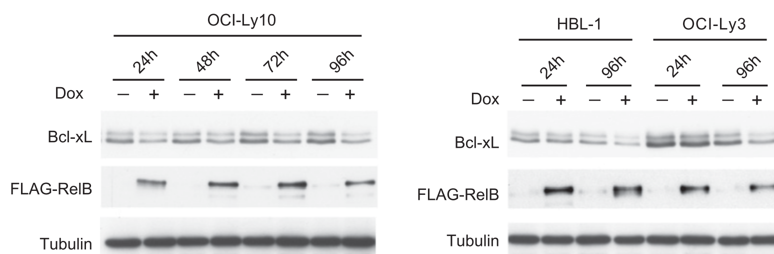

Fig. S9. RelB inhibits expression of the NF-κB target gene Bcl-xL. Expression of FLAG-tagged RelB in DLBCL lines was achieved by retroviral transduction as described previously (1), using cell lines engineered to express the murine ecotropic retroviral receptor for efficient transduction and the bacterial tetracycline repressor for doxycycline-inducible expression. After induction of RelB expression in the ABC DLBCL cell lines OCI-Ly10, OCI-Ly3, and HBL-1 for the indicated times, Bcl-xL levels were assessed by Western blotting.

1. Ngo VN, et al. (2006) A loss-of-function RNA interference screen for molecular targets in cancer. *Nature* 441:106–110.

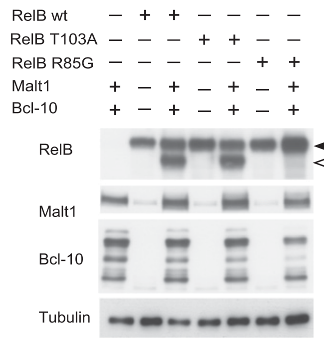

Fig. S10. The RelB mutant T103A is still cleaved by Malt1 in 293T cells. The plasmids encoding the indicated proteins were transfected into 293T cells and postnuclear lysates were analyzed 24 h after transfection by Western blot. Mutation of the phosphorylation site T103 (equivalent to T84 in mouse RelB) did not affect Malt1-dependent cleavage of human RelB. Data are representative of at least two independent experiments.